Preliminary Investigation into Liquid-Cooled PEBBs

J. Padilla, J. S. Chalfant, C. Chryssostomidis, C. M. Cooke
Sea Grant Design Laboratory
Massachusetts Institute of Technology
Cambridge, Massachusetts 02139
Email: jgp7@mit.edu

***Abstract*—This paper describes the design and analysis of a system for removing up to 10 kW of heat from each Power Electronics Building Block (PEBB) in a stack of four PEBB units, using liquid cooling via a dry interface. This is achieved by hard-mounting cold plates in the electronics cabinet, placing the heat-transfer surface of each PEBB adjacent to a cold plate, and improving heat transfer across the interface through the use of a thermal pad. The paper presents initial thermal analysis using analytical models. These analyses indicate that this is a viable solution to the PEBB cooling problem.**

***Index Terms*—Power Electronics, Thermal Management**

I. Introduction

The Navy Integrated Power and Energy Corridor (NiPEC) is a modular entity that encapsulates all the power handling requirements of a shipboard power and energy distribution system including transmission, conversion, protection, isolation, control and storage [1].

The basic component or least replaceable unit of the NiPEC is the Power Electronics Building Block (PEBB), which is envisioned to be a universal converter that is programmed for the specific application when installed [2]. PEBBs may be combined in series or parallel to increase the voltage or current respectively, as required. The NiPEC will contain many, possibly hundreds of, PEBBs, and will provide, among other services, the structural, mechanical and thermal support for the individual PEBBs. An indicative structure for discussion of thermal management is shown in Figure 1.

A PEBB is a modular unit that is designed to be low maintenance, allowing sailors aboard the vessel to easily change out a PEBB with minimal training. All interfaces between the PEBB and the NiPEC must automatically connect and disconnect when the PEBB is inserted and removed, respectively, without any additional adjustment.

Further, there is no liquid connection permitted directly to the PEBB, *i.e.*, liquid may not cross the PEBB boundary. This constraint greatly reduces the possibility of liquids leaking onto the electronics, but is also the constraint that makes thermal management of the PEBB challenging.

This material is based upon research supported by, or in part by, the U.S. Office of Naval Research (ONR) under award number ONR N00014-16-1-2945 Incorporating Distributed Systems in Early-Stage Set-Based Design of Navy Ships; ONR N00014-16-1-2956 Electric Ship Research and Development Consortium; and by the National Oceanic and Atmospheric Administration (NOAA) under Grant Number NA14OAR4170077 - MIT Sea Grant College Program and was approved for public release under DCN # 43-7892-21.

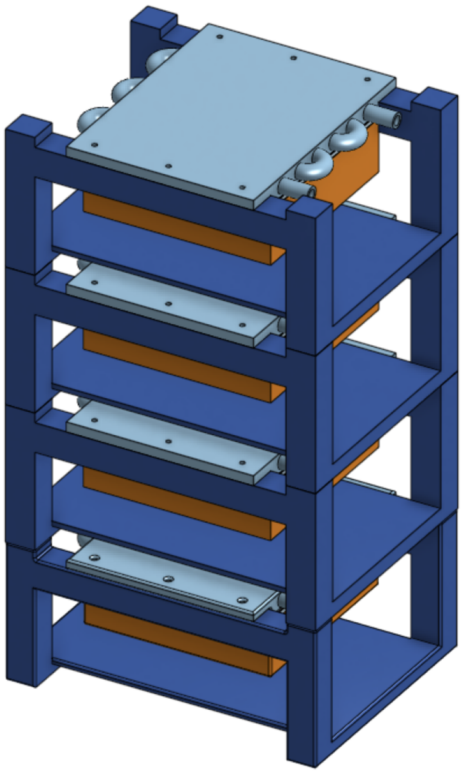

Fig. 1: Example PEBB stack containing the structure, cold plates, thermal pads and PEBBs.

Currently, the thermal management of the PEBB is achieved via a large aluminum finned heat sink, integral to the PEBB and exposed to forced air. The heat is conducted from the heat-producing elements into the heat sink, then convection-cooled by air forced by fans past the fins. The fans, external to the PEBB, are installed in the NiPEC structure. This solution is quite robust and easily implemented for the current power levels in the PEBB; however, the use of air as a working fluid limits the amount of heat that can be removed and thus limits the power level that can be achieved in the PEBB. The low specific heat and density of air, combined with its high viscosity, preclude its use in high-heat-flux applications. In order to achieve significantly greater power density in the same size unit, a more effective heat removal method must be developed.

This paper provides the initial foray into the design and

analysis of a system for removing up to 10 kW of heat from each PEBB, using liquid cooling via a dry interface. This is achieved through a new mechanical design that integrates liquid-cooled cold plates directly into the stack structure of the electronics cabinet seen in Figure 1. These integrated plates enable rigid leak-proof connections to the shipboard cooling system. This design places the outer heat-transfer surface of each PEBB in contact with a cold plate. Thermal pads are employed to reduce thermal contact resistance across the interface between the cold plates and the PEBBs. The analyses presented herein demonstrate that this is a viable potential solution to the PEBB cooling problem.

The remainder of this paper is structured as follows. Section II gives background to the specific application, Section III details the analytical modeling effort, Section IV describes and analyzes several variations to the baseline design, and Section V provides conclusions and discussion of future work.

II. Background

We describe below pertinent details and assumptions necessary to support development of the proposed cooling design.

A. PEBB

The PEBB is designed to be sufficiently small and light to be carried and installed by a single sailor onboard a ship while underway. Thus, the PEBB is constrained to weigh no more than 35 pounds. The total package is approximately 19 inches wide by 19 inches deep by 8 inches tall as currently configured. Although the design has not been completely finalized, the horizontal dimensions are not expected to change significantly; the height may be reduced by the change from air to liquid cooling.

The PEBB shown in Figure 2 is an example configuration amenable to external liquid cooling. The top and/or bottom surfaces are available for transferring heat out of the unit. If a tight connection were to be required on opposing sides of the PEBB, then the NiPEC structure would need to move and the connections to the liquid cooling source would need to flex, introducing an avenue for leaking. Therefore, for this example, we assume that only one surface is used for heat transfer, as a single surface can be mounted to the NiPEC structure without requiring flexibility in the structure.

The main heat-producing elements of the PEBB are a set of 72 switches referred to herein as dice. In a full-bridge configuration, there are 72 dice arranged in groups of six in a single plane as seen in Figure 3 [3].

The exact internal structure of the PEBB sub-components is proprietary, so for the purposes of this study we make the following assumptions:

- The dice are directly mounted to an electrically insulative ceramic material.
- Each die measures 8.1 mm by 8.1 mm with a thickness of 0.5 mm.
- The ceramic layer thickness is assumed to be 7.5 mm, for a total module thickness of 8 mm.

Fig. 2: A sample Power Electronics Building Block (PEBB) [3]. The top and/or bottom surfaces are available for transferring heat out of the unit.

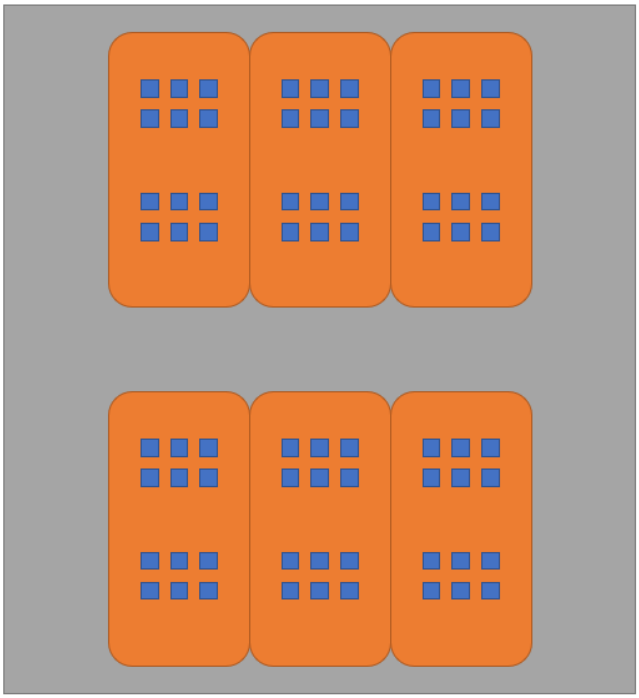

Fig. 3: The die grids assembled into two half-bridges, top and bottom. Blue squares represent dice. Total mounted area, in grey, is 12 inches high by 11 inches wide. [3]

- The ceramic has a thermal conductivity, k, of 180 W/mK, which corresponds to aluminum nitride, a common, electrically insulative, thermally conductive ceramic used in power electronics applications.
- The switch maximum temperature is 175°C. In order to include a safety factor, we use 150°C as the maximum allowed temperature.

B. Thermal Pads

Thermal pads are inserted between an electronic component that needs to be cooled and the cooling solution such as a heat sink to lower the contact resistance by filling in the small gaps between the surfaces when they are placed under a compressive load. This compressive load forces the soft

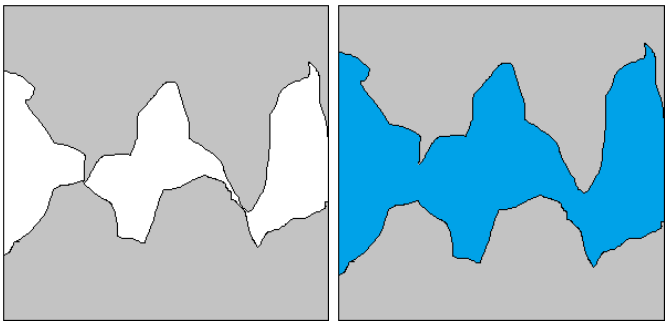

Fig. 4: In the left-hand image, the top and bottom solid grey surfaces touch at high spots, leaving interstitial gaps. In the right-hand image, the blue thermal pad under compression fills gaps, creating improved contact for thermal conductivity.

TABLE I: THERMAL RESISTANCE (R) OF THE TG-A1780 THERMAL PAD UNDER VARIOUS COMPRESSIVE LOADS [4].

Pressure (psi)	R (Cin^2/W)	Deflection (%)
10	0.161	12
30	0.089	18
50	0.071	21

material of the thermal pad to fill the interstitial gaps between the components, supplying a new conductive pathway where an air gap would have been, shown in a representative manner in Figure 4.

An example thermal pad is the t-Global TG-A1780 [4] which has a thermal conductivity of 17.8 W/mK. This pad has a silicone base with thermal conductive powder and flame retardant added. The material has a dielectric breakdown voltage of 4 kV/mm. It is rated at a Shore hardness of 65, which is somewhere between the hardness of a rubber band and a pencil eraser. It comes in thicknesses ranging from 0.5 to 2.0 mm; we select the 2.0 mm pad.

The manufacturer recommends a compressive load between 10 and 30 psi, and provides thermal resistances and pad deflection at these loads as shown in Table I.

C. Cold Plate

One liquid cooling technology commonly used in industry is a cold plate. Cold plates in their simplest form are made of aluminum stock of a desired thickness inlaid with copper piping. A working fluid, commonly chilled water, is pumped through the copper piping before returning to the chiller to be cooled. Advantageous characteristics of cold plates such as low thermal resistance, excellent heat dissipation, and easy customization make them an excellent choice for high-heat-flux systems like PEBBs.

For the initial design, we use a cold plate based on the Boyd Corporation CP12G05 Tubed Cold Plate [5], which consists of 3/8 inch copper tubing embedded in an aluminum plate. This design has a thermal resistance, R, of 0.004 K/W over an area of 60 square inches at a liquid flow rate of 2 gpm.

D. Electrical Isolation

The individual PEBBs must be electrically isolated. In the air-cooled version, this is achieved with an air gap and appropriate stand-off distances. The liquid-cooled version eliminates the air gap, so electrical isolation must be achieved through insulation, either embedded in the PEBB or in the surrounding structure. Since electrically isolating materials also tend to be thermally isolating, one solution is to maintain the cold plate at the same electrical potential as the PEBB, then provide electrical isolation between the cold plate and the NiPEC and ship structure. In this case, electrically isolating fluids such as deionized water or refrigerants must be used.

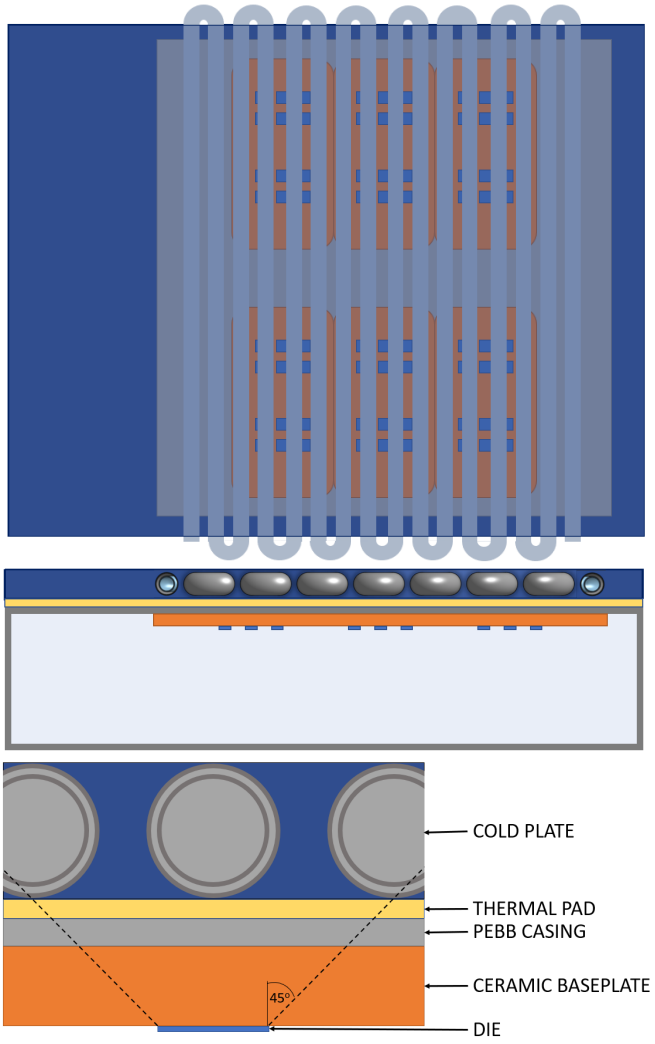

Fig. 5: The dice arrangement relative to the cold plate and thermal pad in plan view (top image) and elevation (middle image). A magnified elevation view is shown in the bottom image. Not to scale.

E. Cooling Solution Overview

The complete cooling solution that incorporates the PEBB, thermal pad, and cold plate is shown in Figure 5. The thermal performance of each proposed design component will be evaluated in Sections III and IV.

III. ANALYTICAL MODELS

The analysis in this section follows traditional heat transfer techniques found in such texts as [6].

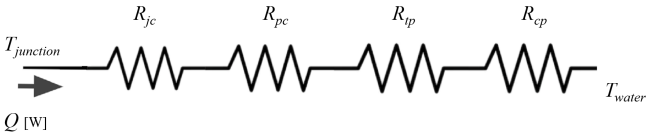

Fig. 6: Thermal resistance network diagram of proposed liquid-cooling system.

The change in temperature from the die to the working fluid is a function of the heat produced in the dice and the thermal resistance of the system such that

$$(T_j - T_f) = \frac{Q}{UA} = QR_{tot} \tag{1}$$

where T_j is the temperature of the die, T_f is the temperature of the working fluid, Q is the heat produced, A is the area across which heat is transferred, and U is the overall heat transfer coefficient. $R_{tot} = 1/UA$ is the total thermal resistance.

To determine the total thermal resistance of the system, a simplified one-dimensional resistance network model is used as shown in Figure 6. This network consists of four main thermal resistances: the resistance of the module, R_{jc}, which quantifies the thermal resistance from the junction of a die to the interior of the PEBB casing; the resistance of the PEBB casing itself, R_{pc}; the resistance of the thermal pad, R_{tp}; and the resistance of the cold plate, R_{cp}.

To understand the one-dimensional thermal resistance models, first it is important to understand the assumptions used to create the model representing the thermal resistance.

A. Thermal Resistance from the Junction to the Case

The thermal resistance between the heat-producing element and the interior of the PEBB casing is R_{jc}, which has been measured in the Virginia Tech CPES laboratory to fall between 0.3 and 0.4 for a single die [3]. We use the worst-case value of $R_{jc} = 0.4\ K/W$.

Another assumption that must be made regards the heat spreading angle within the ceramic. The heat spreading angle determines how the heat spreads in a material from surface to surface. It is commonly used in layered cases such as this one. The heat spreading angle describes the thermal energy's pathway through a material, as seen in Figure 7. We assume a typical heat spreading angle of 45 degrees [7].

B. PEBB Casing

The ceramic baseplate is mounted directly to the 0.1 inch-thick aluminum casing of the PEBB. The thermal resistance through this case for a single die is

$$R_{pc} = \left(\frac{L}{kA}\right)_{pc} \tag{2}$$

where L is the thickness of the PEBB casing, A is the effective critical cross-sectional area, and k is the thermal conductivity of aluminum. We assume the thermal resistance of the transition between the ceramic baseplate and the aluminum casing to be negligible. The resultant R_{pc} is shown in Table IV.

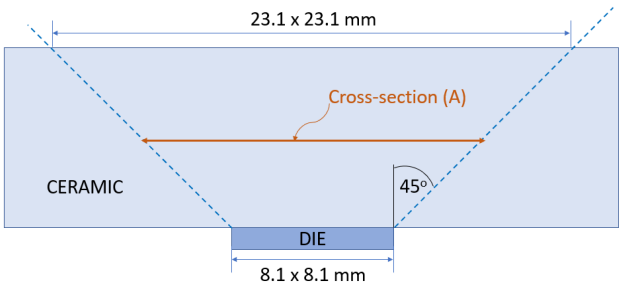

Fig. 7: Heat spreading angle changes effective cross-sectional area as a function of height through a material.

C. Thermal Resistance of the Thermal Pad

Next, the resistance of the thermal pad per die must be determined using

$$R_{tp} = \left(\frac{L}{kA}\right)_{tp}. \tag{3}$$

Assuming a 10 psi compressive load, the 2 mm pad will compress to a 1.76 mm thickness per Table I. Using the thermal conductivity provided by the manufacturer and calculating area using the assumed 45 degree spreading angle yields the thermal resistance shown in Table IV.

D. Thermal Resistance of the Cold Plate

The thermal resistance of the cold plate consists of the resistance of the aluminum plate material, the resistance of the wall of the embedded copper piping, and the resistance of the transition from the solid piping wall to the liquid flowing through the pipe. Our initial cold plate, represented by Figure 8, consists of a single 3/8 inch copper tube embedded in aluminum. Dimensions are provided in Table II.

TABLE II: COLD PLATE DIMENSIONS AND PROPERTIES.

Overall Length	L	in	12
Overall Width	W	in	11
Aluminum Plate Thickness	t	in	0.625
Piping Nominal Size		in	3/8
Piping Outer Diameter	OD	in	0.50
Piping Inner Diameter	ID	in	0.43

1) Heat Transfer Coefficient: A Nusselt number analysis is conducted to determine the heat transfer coefficient from the cold plate structure to the water flowing through it.

The Nusselt number, Nu, is the ratio of convection to conduction across a boundary.

$$Nu = \frac{hD}{k}, \tag{4}$$

where h is the heat transfer coefficient, D is the characteristic length and k is the thermal conductivity of the fluid.

There are a number of empirical relations used to determine the Nusselt number; selection of the proper relation depends on the Reynolds number and Prandtl number of a given application.

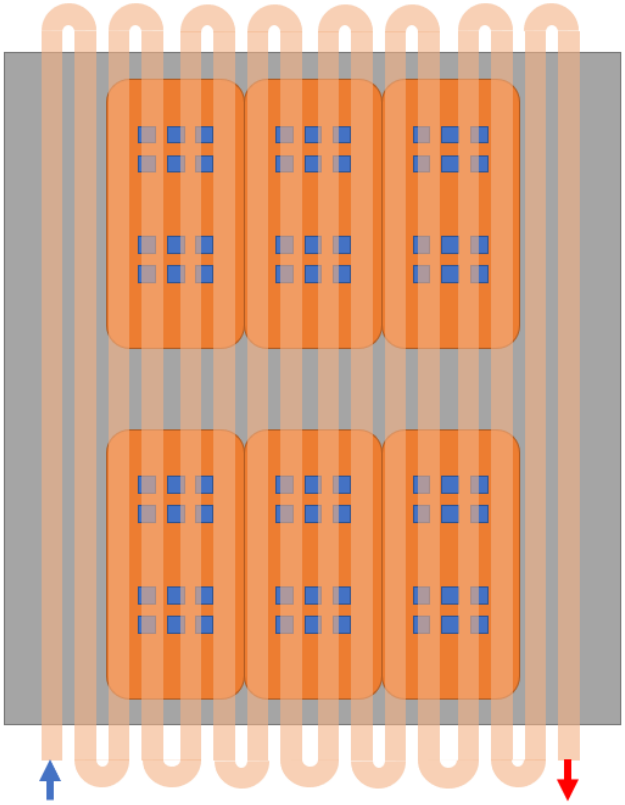

Fig. 8: Initial cold plate piping configuration.

The Reynolds number, Re, is the ratio of inertial to viscous forces in a fluid and is used to determine whether the flow is in the turbulent or laminar regime.

$$Re = \frac{\rho v D}{\mu} \tag{5}$$

where ρ is the fluid density, v is the fluid velocity, μ is the dynamic viscosity of the fluid, and D is the characteristic length which, for this case, is the inner diameter of the tubing. For our application, $Re = 23,608$, indicating turbulent flow; see Table III.

The Prandtl number, Pr, is the ratio of momentum diffusivity to the thermal diffusivity, and is thus an indicator of whether convection or conduction is dominant.

$$Pr = \frac{c_p \mu}{k} \tag{6}$$

where c_p is the specific heat, μ is the dynamic viscosity, and k is the thermal conductivity. Note that the Prandtl number is a function of the fluid only, and is not dependent on the geometry of the application. The Prandtl number for our application is $Pr = 8.2$.

We use the Gnielinski correlation to approximate the Nusselt number for turbulent flow in pipes such that

$$Nu = \frac{(f/8)(Re - 1000)Pr}{1 + 12.7(f/8)^{1/2}(Pr^{2/3} - 1)} \tag{7}$$

TABLE III: PROPERTIES FOR COLD PLATE PERFORMANCE USING WATER AT 15 °C AS THE WORKING FLUID.

Water Properties			
Water Velocity	V	m/s	2.5
Density	ρ	kg/m^3	998.6
Specific Heat	C_p	J/kgK	4191
Dynamic Viscosity	μ	Ns/m^2	1.155
Thermal Conductivity	k	W/mK	0.5891
Prandtl Number	Pr	non-dim	8.2
Cold Plate Properties			
Reynolds Number	Re	non-dim	23,608
Prandtl Number	Pr	non-dim	8.2
Darcy friction factor	f	non-dim	0.0251
Nusselt Number	Nu	non-dim	182
Heat Transfer Coefficient	h	W/m^2K	9863

where f is the Darcy friction factor of the piping, Re is the Reynolds number, and Pr is the Prandtl number. This correlation applies in the range

$$0.5 < Pr < 2000 \text{ and}$$
$$3000 < Re < 5E6,$$

which our application falls within.

The Darcy friction factor, f, is calculated using Petukhov's correlation,

$$f = (0.79(ln(Re) - 1.64))^{-2}. \tag{8}$$

The Nusselt number is determined using equations (5), (6), (7) and (8). Then, equation (4) is used to solve for the heat transfer coefficient of the fluid passing through the piping of the cold plate. Results are shown in Table III.

2) Thermal Resistance: The heat transits the cold plate through the aluminum plate material and the wall of the copper tubing into the working fluid which, in our case, is water. Thus, the thermal resistance is

$$R_{cp} = \left(\frac{L}{kA}\right)_{Al} + \left(\frac{ln(r_o/r_i)}{2\pi Lk}\right)_{Cu} + \left(\frac{1}{hA}\right). \tag{9}$$

where $(A)_{Al}$ is the area of the cold plate; $(L)_{Al}$ is the length of the path traveled in the cold plate aluminum, assumed to be half the thickness of the plate; $(k)_{Al}$ is the thermal conductivity of aluminum; r_i and r_o are the inner and outer radii of the copper tubing, respectively; $(L)_{Cu}$ is the length of the copper tubing within the cold plate, excluding the length outside the aluminum plate required for bends; h is the heat transfer coefficient; and A is the interior surface area of the copper tubing. Details are shown in Table IV.

E. Total Thermal Resistance

Finally, the total thermal resistance of the system, R_{total} can be calculated by adding the resistance of the module, the PEBB casing, the thermal pad and the cold plate together, as resistors in series. Thus, the total resistance for a single die is

$$R_{total} = R_{jc} + R_{pc} + R_{tp} + R_{cp}.$$

TABLE IV: ONE-DIMENSIONAL THERMAL RESISTANCE CALCULATION VALUES, PER DIE

		k (W/m^2K)	h (W/mK)	t (mm)	r_i (mm)	r_o (mm)	L (mm)	A (mm^2)	R (K/W)	R (K/W)
Die	experimental	-	-	-	-	-	-	-		0.4
PEBB Casing	t/kA	205.0	-	2.54	-	-	-	657		0.0188
Thermal Pad	t/kA	17.8	-	1.76	-	-	-	896		0.1103
Plate	t/kA	205.0	-	15.9	-	-	-	1,183	0.0327	
Piping Wall	$ln(r_o/r_i)/2\pi Lk$	385.0	-	-	5.46	6.35	67.7		0.0009	0.0773
Water	$1/hA$	-	9,863	-	-	-	-	2,324	0.0436	
									TOTAL	0.6064

TABLE V: TEMPERATURE PERFORMANCE OF DICE UNDER THREE LOADING SCENARIOS.

	Q $[W]$	R Total $[K/W]$	Δ T $[C]$	T_{max} $[C]$
even distribution	139	0.6064	84	104
80% load	222	0.6064	135	155
20% load	56	0.6064	34	54

F. Temperature Analysis

Using

$$Q = \dot{m}C_p(T_{out} - T_{in}), \tag{10}$$

we find the temperature rise from inlet to outlet of the cooling water to be 10.2 °C for a heat load of Q = 10kW. Assuming an inlet temperature of 10°C, the maximum water temperature is thus 20.2°C. The highest temperature will occur at the die that is correlated in space with the hottest water temperature, which will occur at the bottom right-hand corner of Figure 8.

The PEBB has two main operating scenarios. In the first, the 10 kW heat load is distributed across all 72 dice uniformly such that each die produces a 139 W heat load. In the second scenario, half the dice produce 80% of the heat load and the other half produce 20%, yielding heat loads of 222W and 56W respectively. Note that, in the second scenario, which dice are heavily loaded changes depending on the direction of power flow; a die that sees a 20% load at one time may see an 80% load at another time. Therefore, the cooling system is not biased to cool one set of dice more thoroughly than another.

To see the reaction of the system to such loads, the equation

$$Q = \Delta T / R_{total} \tag{11}$$

is used. Here, Q is the heat load on a single die in Watts, ΔT is the temperature difference between the junction and the water in the cold plate, and R_{total} is the thermal resistance of a single die from junction to cold plate.

Table V shows the results of the system's cooling performance for the load cases. These results show that under all loading scenarios, the die temperature remains below the maximum allowed temperature of 175°C; however, we would prefer to remain below 150°C, so the 80% load scenario is a bit high.

IV. ANALYTICAL MODEL VARIATIONS

In this section, we investigate variations to the cooling solution including variations to the piping diameter, piping arrangement, flow rate, spreading angle, and junction-to-case resistance.

TABLE VI: PROPERTIES AND RESULTS FOR COLD PLATE PERFORMANCE USING WATER AT 15 °C AT A VELOCITY OF 2.5 M/S AS THE WORKING FLUID FOR FOUR DIFFERENT PIPE DIAMETERS.

Nominal Diameter (in)	1/4	3/8	1/2	1
Fluid Properties				
Reynolds Number	17,294	23,608	29,921	56,274
Prandtl Number	8.2	8.2	8.2	8.2
Darcy friction factor	0.0272	0.0251	0.0237	0.0204
Nusselt Number	139	182	225	390
Heat Transfer Coef (W/m^2K)	10,222	9,863	9,580	8,824
Heat Transfer Properties				
Tot. Thermal Resistance (K/W)	0.5927	0.6064	0.6184	0.6589
Temperature at 80% load (°C)	161	155	154	158
Temperature at 20% load (°C)	62	54	51	48
Temp. even distribution (°C)	111	105	102	103
Piping Properties				
Volumetric Flow Rate (gpm)	2.0	3.7	6.0	21.1
Equivalent Length (m)	16.6	13.2	11.4	8.6
Pressure Loss (kN/m^2)	175	94	61	21
Pump Power (W)	22.1	22.1	22.9	28.0

A. Piping Diameter

We investigated the impact of changed piping diameter by analyzing cold plates made with piping of diameters 1/4, 1/2 and 1 inch in addition to the 3/8 inch piping described above. Figure 9 represents two of these versions, in which one can see the change in number of passes with change in piping diameter. The number of passes was controlled by the overall plate width and the piping diameter. The results of the Nusselt number analysis for each piping size are provided in Table VI.

A further evaluation is the pumping power required for different diameter piping. For a run of straight piping, the pressure loss due to friction on the sides of the pipe, Δp, can be calculated using the Darcy-Weisbach equation

$$\Delta p = \frac{1}{2}\frac{L}{D}\rho v^2 f \tag{12}$$

where ρ is the density of the water, v is the water velocity, f is the Darcy friction factor calculated in (8), and D is the inner diameter of the piping.

The pressure loss in fittings is calculated using an equivalent length factor, $(L/D)_{eq}$. factors used are

$$(L/D)_{eq} = 50 \text{ for } 180^\circ \text{ bend}$$
$$(L/D)_{eq} = 5 \text{ for piping entry and exit.}$$

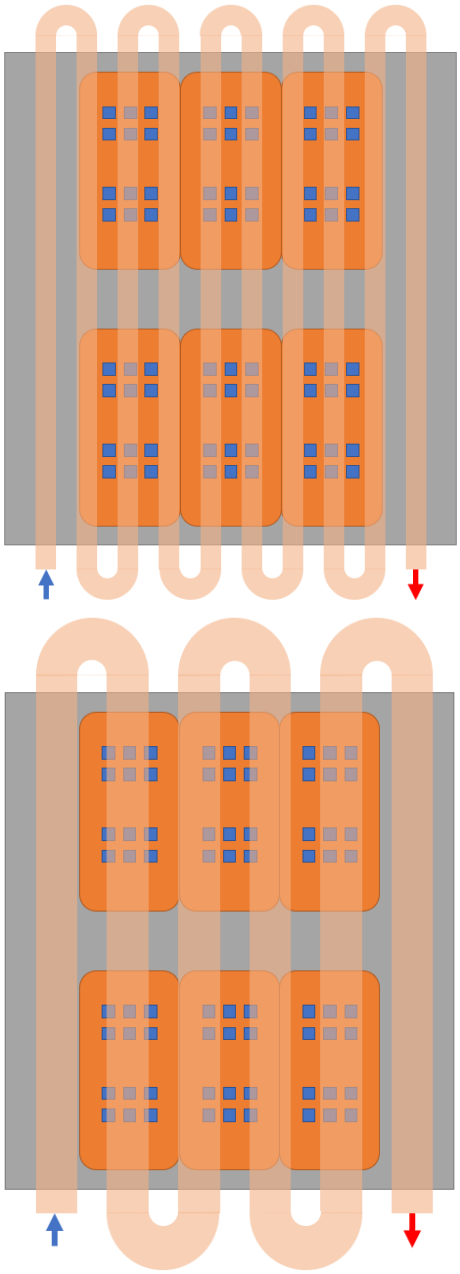

Fig. 9: Cold plates with varying pipe diameters. The top image shows 1/2 inch piping, and the bottom image shows 1 inch piping.

Multiplying this factor by the number of fittings and the diameter of pipe yields an equivalent length which is added to the straight pipe run length for use in (12).

Pump power required to overcome the head loss in the cold plate only, excluding the piping system leading to the cold plate, is then calculated to be

$$P = \dot{v}\Delta p. \tag{13}$$

where $\dot{v}$ is the volumetric flow rate.

The volumetric flow rate, total length including equivalent length, pressure loss and pump power for the four piping sizes

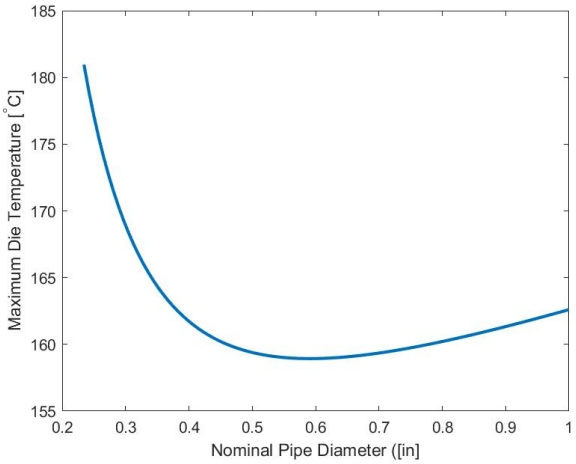

Fig. 10: Variation of maximum die temperature with piping diameter.

are displayed in Table VI. Note that pressure drop in fittings tends to decrease with increased pipe diameter, so the pressure loss and pump power are most likely underestimated for the 1/4 inch piping and overestimated for the 1 inch piping, but the numbers shown are indicative of the trends.

As a thought exercise, the diameter of the piping in the plate was varied continuously with a continuous and thus non-integer number of passes, neglecting the resistance within the copper pipe wall. This yields the correlation shown in Figure 10, which indicates a peak performance for this application in the neighborhood of 1/2 inch piping. As an intuitive exploration of this phenomenon, we recognize first that since we have selected a constant water velocity regardless of pipe size, increased pipe diameter increases the amount of water and thus decreases the maximum water temperature. Countering this effect is the increased resistance of the cold plate due to an increased average distance that heat travels through the cold plate with increased pipe diameter, and a slight decrease in heat transfer rate to the water at higher diameters.

B. Counter-Flow Heat Exchanger

The performance of the cold plate will improve if the cold plate is arranged as a counter-flow heat exchanger rather than a single-pass arrangement. As an example, see the cold plate in Figure 11. Note that this consists of several loops, and the cold water inlets are interleaved with the hot water outlets. Whereas the total thermal resistance of this arrangement is the same as that of a single-pass version, the maximum temperature of the water is lower; since any one die is exposed to multiple loops, an average temperature is used to determine heat transfer.

The counter-flow heat exchanger temperature results are provided in VII. There are several items to note. First, the counter-flow heat exchanger achieves a lower maximum temperature per die than the baseline cold plate; the maximum temperature is now below our goal of 150°C for even the 80% load scenario for all the smaller piping diameters. Further, the minimum temperature is achieved at a smaller piping diameter

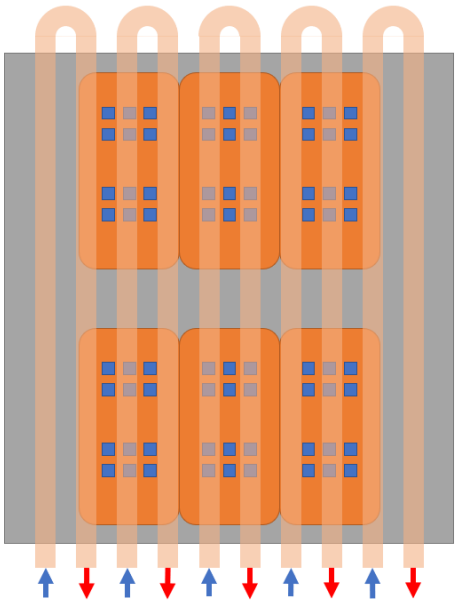

Fig. 11: Cold plate arranged as a counter-flow heat exchanger.

TABLE VII: RESULTS FOR VARIOUS PIPING DIAMETERS IN A COUNTER-FLOW HEAT EXCHANGER. THE BOTTOM ROW IS THE ORIGINAL SINGLE-PASS DESIGN FOR COMPARISON. TEMPERATURES ARE PROVIDED FOR THE THREE OPERATING SCENARIOS: T_1 AT 80% LOAD, T_2 AT 20% LOAD AND T_3 AT UNIFORM LOAD, ALONG WITH TOTAL THERMAL RESISTANCE PER DIE AND FLOW RATE AND PUMPING POWER FOR THE COLD PLATE.

Diameter (in)	T_1 (°C)	T_2 (°C)	T_3 (°C)	R_{tot} (K/W)	Flow Rate (gpm)	Pump Power (W)
1/4	143	44	93	0.5927	23.9	17.4
3/8	145	44	95	0.6064	29.7	17.0
1/2	148	45	96	0.6184	35.8	17.3
1	157	47	102	0.6589	63.3	21.2
Baseline	155	54	104	0.6064	3.7	22.1

than in the baseline. Second, pumping power is reduced due to fewer restrictions in the piping, but flow rate has increased significantly. Third, the total thermal resistance per die is the same as the single-pass cold plate at the same piping diameter, so all temperature savings are the result of the water flow.

C. Flow Rate

Using the counter-flow heat exchanger with 3/8 inch piping, we varied the flow rate from 1.0 m/s to 3.0 m/s. The results are shown in Figure 12. Once can see that there are diminishing returns in temperature decrease for the increase in flow rate at the higher velocities.

D. Reduced Spreading Area

One area of great uncertainty in our estimates of thermal resistance is the common assumption of a 45 degree spreading angle. Guenin [7] indicates that the assumption may be accurate within 10 percent for our application. We looked at the impact of this assumption by reducing the spreading area by 10 percent, and by reducing the spreading angle to 30

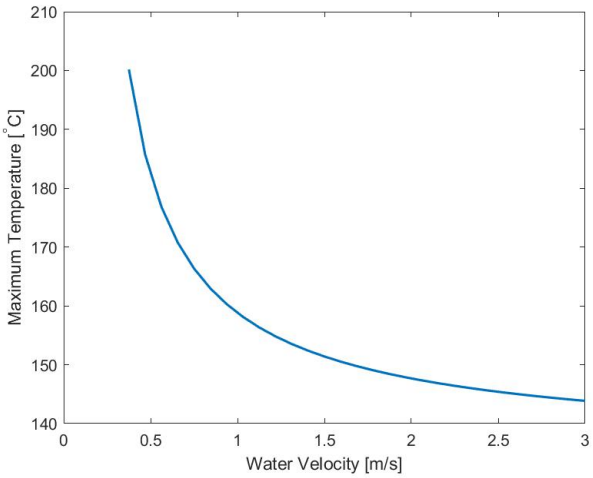

Fig. 12: Change in maximum die temperature with variation in water velocity.

TABLE VIII: RESULTS FOR CHANGES TO SPREADING ANGLE AND TO JUNCTION-TO-CASE RESISTANCE, AS COMPARED TO THE BASELINE. TEMPERATURES ARE PROVIDED FOR THE THREE OPERATING SCENARIOS: T_1 AT 80% LOAD, T_2 AT 20% LOAD AND T_3 AT UNIFORM LOAD. THE FINAL COLUMN IS THE TOTAL THERMAL RESISTANCE PER DIE.

Case	T_1	T_2	T_3	R_{tot}
Baseline				
Baseline (3/8 inch piping)	155	54	104	0.6064
Spreading Angle				
Reduce spreading area by 10%	160	55	107	0.6272
30 degree spreading angle	186	62	124	0.7451
Junction-to-Case Resistance				
$R_{jc} = 3.0\ K/W$	133	48	91	0.5064

degrees. The change in temperatures and in thermal resistance for these cases are shown in Table VIII. The impact can be fairly significant. This warrants further investigation through simulation and experimentation.

E. Reduced Junction-to-Case Resistance

As stated earlier, we assume the worst case scenario of junction-to-case thermal resistance in which $R_{jc} = 4.0$; however, experiments at VA Tech have achieved resistances below that. If we assume $R_{jc} = 3.0$, the maximum temperatures of the dice are well below the goal. Using a single-loop cold plate with 3/8 inch piping, the maximum temperature at the 80% loading scenario is 133°C. See Table VIII.

V. CONCLUSIONS AND FUTURE WORK

This paper has provided initial thermal analysis of a liquid-cooled PEBB with dry interface. The analysis demonstrates that the proposed method is a potential viable solution to removing up to 10kW of heat from the PEBB. Numerous areas of further research exist.

Use of a counter-flow heat exchanger cold plate along with a thermal pad provides a realistically achievable solution.

Additional research into optimizing the heat exchanger is expected to yield an even further improved cooling solution. The analytical results require verification through simulation and experimentation; both are planned as next steps in the process.

Structural analysis of the PEBB under load is required.

One open question is the robustness of this solution to mechanical disturbances such as misalignment of the PEBB and cold plate, or the intrusion of some small obstruction or grit between the thermal pad and the cold plate. Another area of inquiry is the long-term performance of the thermal pad. Additional testing and simulation is required in these areas.

The majority of the thermal resistance in the system is within the PEBB itself, which offers the best area for further reduction of thermal resistance. As an example, employing vapor chambers built into the PEBB could spread the heat over a greater surface area, making the heat removal more feasible. The cooling solution proposed herein uses only a portion of one side of the PEBB. There is space for a much larger cold plate, and potential for use of the other side of the PEBB for cooling as well, should it prove feasible to spread the heat over a greater area.

Electrical isolation of the PEBB and cold plate from the NiPEC structure is envisioned to be achievable through the use of deionized water in the cold plate and non-conductive liquid connections. Further research into electrical isolation of the cold plate is required.

REFERENCES

[1] C. Cooke, C. Chryssostomidis, and J. Chalfant, "Modular integrated power corridor," in *Electric Ship Technologies Symposium (ESTS), 2017 IEEE*. IEEE, 2017, pp. 91–95.

[2] T. Ericsen, N. Hoingorani, and Y. Khersonsky, "PEBB – power electronics building blocks from concept to reality," in *IEEE Petroleum and Chemical Industry Technical Conference 2006 (PCIC06)*. IEEE, September 11-13, 2006, paper PCIC-2006-22.

[3] S. Mocevic, J. Yu, Y. Xu, J. Stewart, J. Wang, I. Cvetkovic, D. Dong, R. Burgos, and D. Boroyevich, "Power-cell design and assessment methodology based on a high-current 10 kV SiC MOSFET half-bridge module," *IEEE Journal of Emerging and Selected Topics in Power Electronics*, pp. 1–1, 2020.

[4] T-Global Technology Co., Ltd., "TG-A1780 Ultra Soft Thermal Pad," Brochure, 2020.

[5] Boyd Corporation, "CP12G05 Tubed Cold Plate," Brochure, 2020.

[6] F. P. Incropera, D. P. Dewitt, T. L. Bergman, and A. S. Lavine, *Introduction to Heat Transfer*, 5th ed. John Wiley & Sons, 2007.

[7] B. Guenin, "The 45° heat spreading angle – an urban legend?" *Electronics Cooling*, vol. 9, no. 4, November 2003.